Estimation of Radio Refractivity Structure using Radar Clutter

Peter Gerstoft[1], *L. Ted Rogers*[2], *Lee J. Wagner*[2], *and William S. Hodgkiss*[1]

[1]Marine Physical Laboratory, University of California San Diego, La Jolla, CA 92093-0238 USA
[2]Atmospheric Propagation Branch, SPAWAR Systems Center, San Diego, CA 92152 USA

Abstract–**This paper describes the estimation of low-altitude atmospheric refractivity from observations of radar sea clutter. Both surface and evaporation ducts are considered. The intended use of the technique is to provide near-real-time estimation of ducting effects for naval forces, which is important for radar performance prediction.**

For surface duct inversions, we use the Simulated Annealing / Genetic Algorithm (SAGA) general purpose inversion code. SAGA is configured to use an embedded parabolic equation electromagnetic propagation model, a four-parameter model for atmospheric refractivity, and a linear least-squares objective function. The mismatch between (a) the optimal replica field and the observed clutter and (b) the inferred refractivity profile and the range-dependent refractivity structure obtained by *in situ* measurements, is discussed.

The inference of evaporation duct heights is simpler than the inference of surface duct parameters and has already been presented in the open literature. The material presented here is an update on the performance of the algorithm based on recent at-sea testing.

I. INTRODUCTION

Low-altitude atmospheric refractive conditions significantly affect the performance of shipboard radars. This can be due to either evaporation ducts or surface ducts, see Fig. 1. Surface ducts appear about 15% of the time worldwide and 25 % of the time off Southern California coast and 50 % of the time in the Persian Gulf [1]. Surface-based ducts are less common than evaporation ducts, but their effects are often more dramatic. They often manifest themselves in a radar's plan position indicator (PPI) as clutter rings (see Fig. 3) and they result in significant height errors for 3-D radar as the lowest elevation scans become trapped on the surface instead of refracting upward as would be expected for a standard atmosphere. Surface based ducts are usually associated with either the capping inversion of the marine atmospheric boundary layer (MABL) or thermal boundary layers, neither of which are characterized by the by surface layer models such as LKB and associated point measurements.

The first description of estimating surface-based duct structure from radar clutter observations using modern tools was by Krolik *et al.* [2, 3]. They formulated the refractivity-from-clutter (RFC) problem as a maximum likelihood (ML) problem using a vector of global refractivity parameters and log-amplitude data as obtained from a radar. The work in this paper supports determining which global parameters (which can include parameters describing range-dependency) should

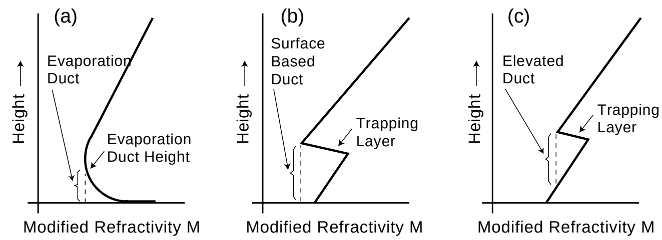

Fig. 1. *Modified refractivity M versus height. (a) Evaporation duct. (b) Surface-based duct. (c) Elevated duct. The modified refractivity is the refractivity multiplied with* 10^6 *and corrected for the curvature of the earth.*

be used in RFC. Surface duct inversions are covered in Sec. II.

Evaporation ducts are a ubiquitous feature of marine environment that usually increases the range at which low-altitude targets can be detected. Evaporation ducts are features associated with the marine surface layer and surface layer models such as that of *Liu, Katsaros and Businger* (LKB) [4] can map shipboard point-measurements of air temperature, sea temperature, relative humidity and wind speed into a refractivity profile from which – along with the appropriate radar and target model – the performance of the radar can be determined. A method for the inference of evaporation duct heights from radar sea clutter was reported in [5]. Recent results in applying the inversion algorithm to data from a U.S. Navy cruiser are covered in Sec. III.

II. SURFACE DUCT INVERSION

From [5], The clutter power p (in dB) in the absence of receiver noise, can be modeled as

$$p(r,\mathbf{m}) = -40\log f(r,\mathbf{m}) + 10\log(r) + C \qquad (1)$$

where f is the one-way propagation loss as modeled using the Terrain Parabolic Equation Model (TPEM) [6]. C is an offset that takes into account radar parameters and the radar sea clutter cross section (σ°). σ° is assumed to be range-independent. Krolik *et al.* found improved results by allowing some compliance for range-dependency in σ°, however, it is not possible yet to draw a general conclusion as to if, or how much compliance is useful. The elements of $\mathbf{m}$ correspond to the four refractivity parameters illustrated in Fig. 2.

Replica vectors are calculated from Eq. (1) to obtain, $\mathbf{p}(\mathbf{m}) = \{p_c(\mathbf{m},r_1),\cdots,p_c(\mathbf{m},r_N)\}$. C is adjusted so the average power of the replica vector (dB) has the same average

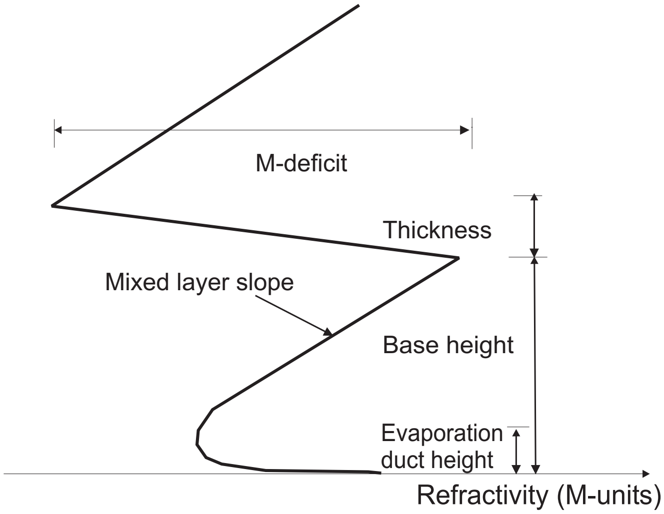

Fig. 2. *Refractivity model*

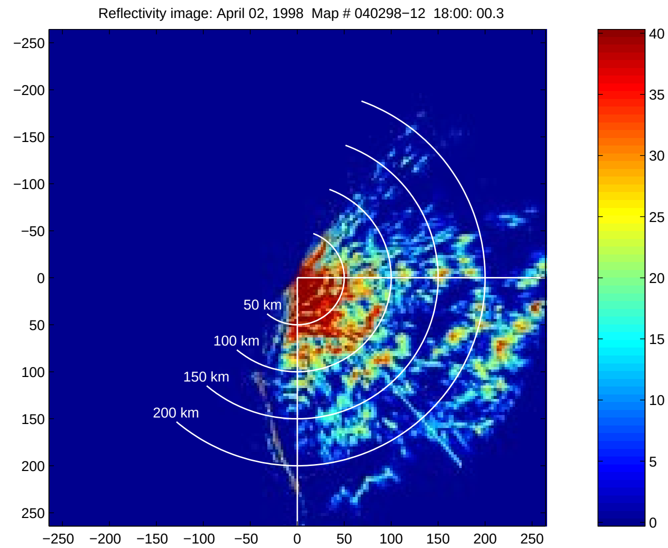

Fig. 3. *Clutter map from SPANDAR corresponding to Wallops Run 12.*

power as the observed clutter power **q**. As with the radar data, all observed data **q** below 0 dB are cut off. Therefore, when adjusting the mean, the replica is also cut-off at 0 dB. A simple least squares objective function is used for optimization of the unknown refractivity profile parameter vector **m**:

$$\phi(\mathbf{m}) = \sum_{i=1}^{N} [p_i(\mathbf{m}) - q_i]^2 = (\mathbf{p}-\mathbf{q})^{\mathrm{T}}(\mathbf{p}-\mathbf{q}). \qquad (2)$$

A. Experimental data

Radar and *in situ* validation data were obtained during the Wallops '98 measurement campaign [5] conducted by the Naval Surface Warfare Center, Dahlgren Division. The data presented here are from the surface-based ducting event that occurred on April 2, 1998. Radar data were obtained using the Space Range Radar (SPANDAR). The antenna height for the SPANDAR is 30.8 meters and clutter maps were taken with the antenna elevation angle set to 0°. All other parameters were set to values given in [5], except pulse width which was set to 2 μsec. A clutter map from the ducting event is shown in Fig. 3.

Meteorological soundings were obtained by an instrumented helicopter provided by the Johns-Hopkins University Applied Physics Laboratory. The helicopter would fly in and out on the 150° radial from a point 4 km due east of the SPANDAR. During the flights, the helicopter would fly a saw-tooth up-and-down pattern. Contour plots of refractivity versus range and height are shown in Fig. 4. Dark lines superimposed on the plot are the modified refractivity profiles. The waveguide can be seen in the first 100 m. The earlier profiles show substantial range dependency.

B. Sensitivity

Figure 5 shows the modeled clutter returns, Eq. (1), as a function of range (x-axis) and variation of individual parameters (y-axis). Clearly, changes in the inversion base height (z_T), thickness (Δz) and mixed layer slope (dM/dz) shift the location of intensifications. Additionally, the size of the horizontal

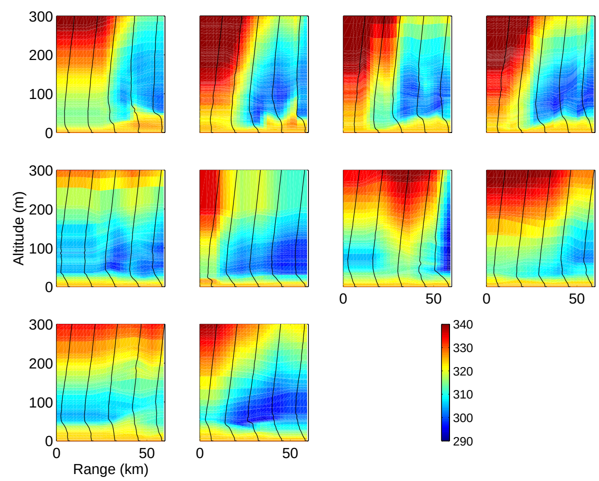

Fig. 4. *Refractivity profiles (in M-units) sequenced in time. The first row is observed from 13:47–15:26, middle 17:26–19:15 and bottom 21:00–21:52. All refractivity profiles have the same value at sea level.*

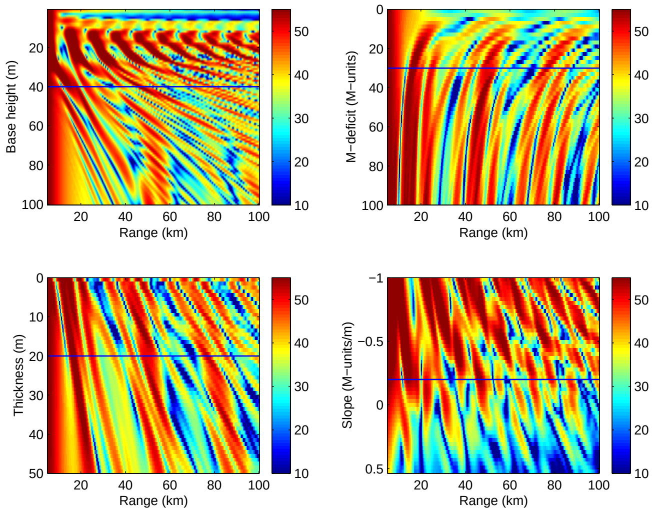

Fig. 5. *Sensitivity to varying environmental parameters of the clutter return. The plot shows the clutter power return (Eq. 1). The horizontal line indicates the baseline value held fixed while the other parameters are varied.*

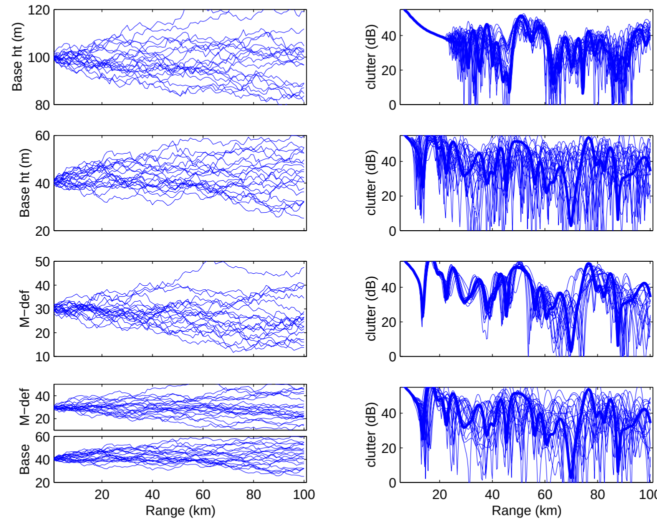

Fig. 6. *Simulation of clutter return based on a Markov chain random variation in a parameter for 20 realizations. a) Variation in base height from 100 m, b) variation in base height from 40 m, c) variation in M-deficit from 30 M-units, and d) variation in both base height from 40 m and M-deficit from 30 M-units. The thick line in the clutter profile is based on the range independent baseline profile.*

shift in the location of an intensification increases nearly linearly as a function of the intensification's original range. One might hypothesize that in performing the inversions, one is really inverting a super-parameter that is a linear combination of of z_T, Δz and dM/dz. As long as a surface duct is created, the M-deficit (ΔM) is not an important parameter. In the present simulation, this happens for an an ΔM value of about 20-30 M-units. With a negative slope in the mixed layer, a surface channel will always be created causing high clutter return. But for positive slopes, the creation of surface duct depends on the z_T, Δz and ΔM.

From the refractivity profiles in Figure 4, it is clear that the refractivity profiles show a range dependence that is somehow random in nature. This effect is simulated by modeling variations in range as a Markov process as shown in Fig. 6. For each kilometer, the profile was updated using a Gaussian distribution with a standard deviation of 1 (m or M-units).

In the top pair of plots in Fig. 6, the random variations in z_T about the starting value of 100 m provide some corruption to the major intensification between 45 and 60 km, but the intensification is still recognizable. On the other hand, in the second pair of plots where the variations are about a starting z_T value of 40 meters, features occurring beyond about 30 km, are difficult to associate with the features in the horizontally homogeneous case. This illustrates the state-dependence of the response to parameter variations. Clearly the random variations in ΔM do not introduce as much variability as those in the base height. The lowest plots correspond to joint, independent variations in the ΔM and base height. The variability is dominated by that induced from the base height.

In Fig. 7 are plotted the envelopes and median values of clutter return data from the SPANDAR. The upper series of plots corresponds to envelopes over different 5-degree sectors from the same clutter map. Plots in the lower series correspond to envelopes over a single 5-degree sector that were obtained at 10-minute intervals. The horizontal broadening of the envelopes with respect to range possibly is explained either by variations in the mean value (with respect to range) of the parameters (of which Fig. 5 illustrates a case), or by random variations in range as illustrated in Fig. 6.

C. Real Data Results

An example of the inversion result is given in Fig. 8. The Simulated Annealing / Genetic Algorithm code [7, 8] is used to optimize (2) where the observed clutter data ($\mathbf{q}$) is taken from the 150° radial from 10 km to 60 km from the clutter map shown in Fig 3. Observations on these results are as follows:

1. The inferred refractivity profile indicates a low surface based duct as do the observed profiles shown in Fig. 4.

2. The match between the observed clutter data ($\mathbf{q}$) and the optimal replica field $\mathbf{p}^*$ is better than the match between observed radar clutter data and $\mathbf{p}^{\mathrm{Met}}$, where $\mathbf{p}^{\mathrm{Met}}$ is modeled based on the measured refractivity field from the helicopter. This suggests that—at least close to the surface—$\mathbf{m}^*$ is more representative than the environment determined from *in situ* measurements.

3. There is some displacement in range as to where peaks and minimums appear in $\mathbf{p}^*$ as compared to where they appear in $\mathbf{q}$ and the displacement is non-uniform. Such a shifting of features is problematic for the squared-error processor $\phi(\cdot)$. Before the variations in horizontal displacements begin to approach half of the the distance from peak-to-peak, minimizing $\phi(\cdot)$ will begin favoring smoother replicas ($\mathbf{p}$'s). As can be ascertained from Figs.

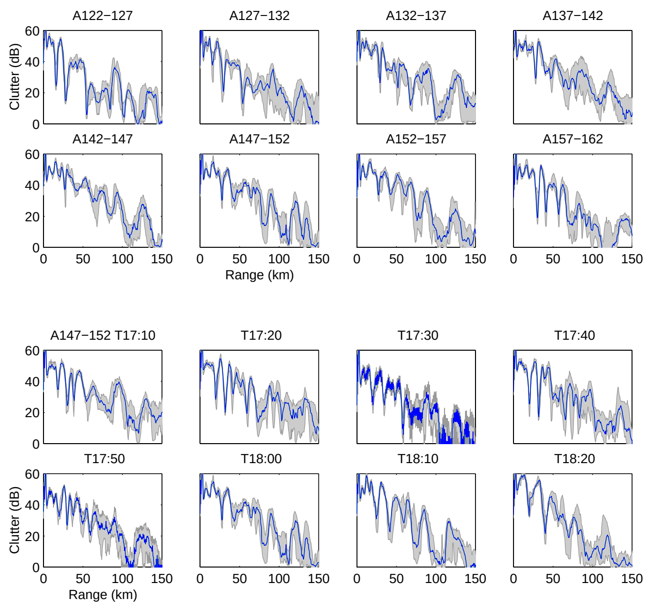

Fig. 7. Clutter return as a function of range for different angles (top) and time (bottom). The shaded area is the envelope of 15 returns in a 5-degree interval and the dark line is the median. In the top figure the 5-degree angle intervals for azimuths centered at 125–160 degrees at time 18:00. In the bottom figure, the time interval is 17:10–18:20.

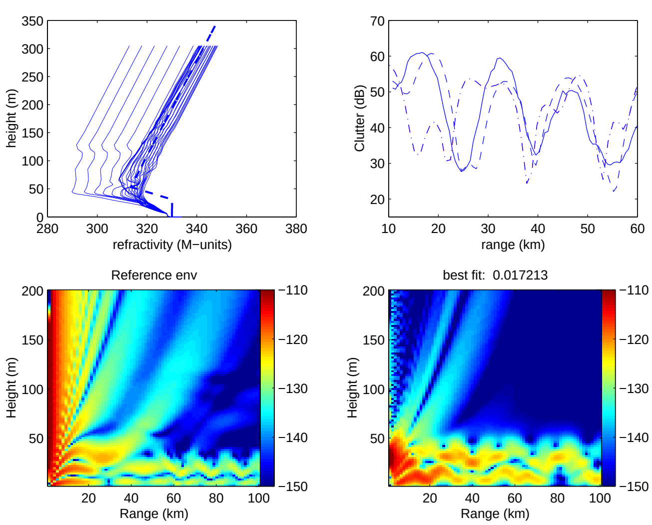

Fig. 8. *Example of inversion result. (top left): Estimated refractivity profile (dashed) based on a range-independent model, the profiles measured by the helicopter Run 7 are shown as thin lines. (top right): The clutter return as observed by the radar data (solid), the modeled return using the inverted profile (dashed), and the modeled clutter return for the helicopter run is shown (dash-dotted). (bottom left): The reference coverage diagram based on the profiles from helicopter Run 7. (bottom right): The coverage diagram based on inverted profile.*

5 and 6, either a lowering of the duct or increasing the range (in km) used in **q** would exacerbate the problem.

4. The coverage diagrams show that while both the inverted environment indicate trapping substantial energy within the first 50 meters, the location of nulls and intensifications in the two environments are uncorrelated. Also, the clutter strength is not included in the inversion, thus the absolute level in the coverage diagrams can differ.

III. EVAPORATION DUCT HEIGHT ESTIMATION

Rogers *et al.* [5] simplified the radar equation from Barton [9] to the following expression for radar clutter power P_c at range r referenced to the power at range r_0 as a function of the evaporation duct height δ

$$\begin{aligned}\Delta_{P_c}(r,r_0,\delta) &= P_c(r,\delta) - P_c(r_0,\delta)\\ &= 10\log\left[\frac{f(\delta,r)^4 r_0^4}{f(\delta,r_0)^4 r^4}\right] + k\,10\log\left[\frac{\psi(r,\delta)}{\psi(r_0,\delta)}\right]\\ &+\ 10\log\left[\frac{r}{r_0}\right] + [\sigma^\circ_E(E(r)) - \sigma^\circ_E(E(r_0))]. \quad (3)\end{aligned}$$

where $f(\cdot)$ is the propagation factor, k is the dependence of the sea clutter radar cross section on the grazing angle ψ (itself a function of the environmental conditions), and σ°_r is the component of the radar cross section of the sea surface that is independent of the grazing angle. In absence of *a priori* information, is is reasonable to assume $[\sigma^\circ_E(E(r))$ - $\sigma^\circ_E(E(r_0))] = 0$.

The clutter power referenced to its value at 12 km, as a function of range for an S-band system (3 GHz) and an antenna height of 30 meters is shown in Figure 9. The lines on the plot are parametric in duct height. Two sets of lines are presented that correspond to grazing angle dependencies of ψ^0 and ψ^4. Presently there is some debate as to grazing angle dependency for vertical polarization [10]. The grazing angle debate notwithstanding, it is clear that the signal for the evaporation duct is embedded in the slope of the clutter power.

Rogers *et al.* [5] reported on testing the evaporation duct algorithm using data from the Space Range Radar (SPANDAR) at Wallops Island, Virginia. Since that time, the duct height estimation algorithm has been applied to data collected during the At-Sea Demonstration of Lockheed-Martin's Tactical Environmental Processor (TEP). TEP is a system for obtaining weather-radar output from the SPY-1 radar installed on U.S. Navy cruisers and destroyers.

In practice, the duct-height estimation routine consists of five steps: (1) quality control to remove point targets, rain, etc., (2) median filtering to remove sea-spikes, (3) azimuthal averaging to mitigate large-scale spatial variability of the sea clutter radar cross section, (4) determination of the initial and final ranges of the observed clutter to use in the least-squares inversion algorithm, and (5) performing the inversion by finding the modeled $P_c(r)$ having the best fit to the processed clutter data.

The most extensive testing was onboard the USS Normandy (CG-60) in the time period of May 10^{th} through May 17^{th}, 2000, off the eastern seaboard of the United States. During

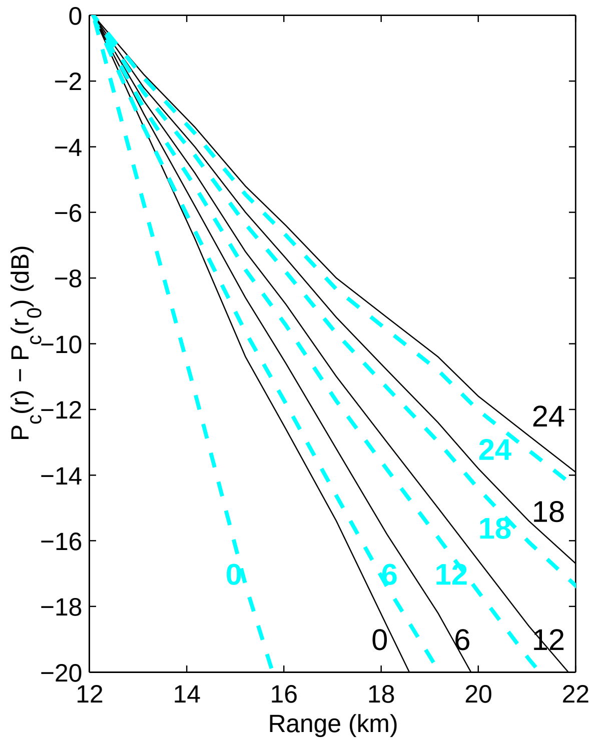

Fig. 9. *Clutter power with respect to range referenced to value at r_0 = 12 km, parametric in evaporation duct height. Solid lines correspond to $\sigma^\circ \propto \psi^0$ and dashed lines correspond to $\sigma^\circ \propto \psi^4$.*

that test, shipboard observations of air temperature, sea-surface temperature, wind speed and relative humidity were recorded at roughly 1-hour intervals for up to 16 hours daily. During some portions of each day, the TEP system generated clutter maps. Valid events are occasions where both a clutter map and meteorological observations occurred within 15 minutes of one another. All valid events are shown in Figure 10.

The ground truth for the evaporation duct height calculations is the value calculated by inputting the meteorological observations into the LKB model [4]. The match between the radar-inferred and LKB-estimated duct heights are close except for the 9^{th}, 10^{th} and 23^{d} events. For these cases, the air-sea temperature differences and Monin-Obukhov lengths are positive, conditions that are problematic for LKB [11, 12].

Event 28 is the only apparent failure for the algorithm. For this case the wind speed is quite low (2–3 m/s). This brings up the issue of availability. The sea-clutter radar cross section is generally an increasing function of the wind speed. To implement the evaporation duct algorithm, it is necessary to be able to observe clutter (a) at ranges over which the slope of the clutter power is affected by the evaporation duct, and (b) over a sufficient range to mitigate the effects of noisy nature of the clutter returns. Thus there will exist a threhold wind speed below which the inversion algorithm cannot be used. One of our goals for the future is to obtain data at lower wind speeds to firmly establish the availability of the algorithm.

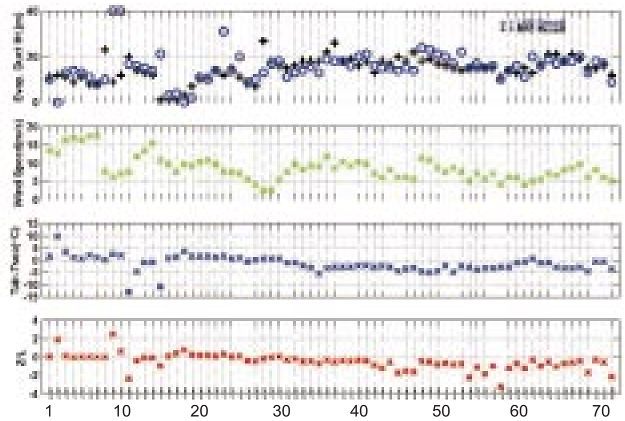

Fig. 10. *Event series from measurements onboard USS Normandy (CG-60). The upper panel show δ calculated using bulk inputs to the LKB model (blue O) and inferred by the radar (black +), respectively. The remaining plots shows the wind speed, the air-sea temperature difference and the Monin-Obukhov length (Z/L).*

IV. SUMMARY

Algorithms for estimating refractivity from clutter has been described for evaporation ducts and surface ducts. The evaporation duct appears much simpler as it only involves estimating one parameter.

Acknowledgments

Funded by the Office of Naval Research Codes 321 and 322.

V. REFERENCES

[1] Patterson, W., Ducting Climatology Summary, software available from: Space and Naval Warfare Systems Center, Code D858, San Diego, CA, 92152–7385, Jan. 1992.

[2] Krolik, J.L. and J. Tabrikain, Tropospheric refractivity estimation using radar clutter from the sea surface, *Proc. 1997 Battlespace Atmospherics Conference,* SPAWAR Systems Command Tech. Rep. 2989, pp. 635-642, March, 1998.

[3] Krolik, J.L., J. Tabrikian, S. Vasudevan and L.T. Rogers, Using radar sea clutter to estimate refractivity profiles associated with the capping inversion of the marine atmospheric boundary layer, *Proc. of IEEE 1999 International Geoscience and Remote Sensing Symposium, Hamburg, Germany,* 28 June - 2 July, 1999.

[4] Liu, W.T., K.B. Katsaros, and J.A. Businger, "Bulk parameterization of air-sea exchanges of heat and water vapor including molecular constraints on the interface," J. Atmospheric Sci., 36, 1722-1735, 1979.

[5] L.T. Rogers, C.P. Hattan, J.K. Stapleton, "Estimating evaporation duct heights from radar sea clutter," *Radio Science*,35(4), pp. 955-966, Jul.-Aug., 2000.

[6] A.E. Barrios, "A terrain parabolic equation model for propagation in the troposphere," *IEEE Trans. Antennas Propagat.*, vol. 42, pp. 90–98, Jan. 1994.

[7] P. Gerstoft, "SAGA Users guide 2.0, an inversion software package," SACLANT Undersea Research Centre, SM-333, 1997. http://www.mpl.ucsd.edu/people/gerstoft/saga.

[8] P. Gerstoft, D.F. Gingras, L.T. Rogers and W.S. Hodgkiss, "Estimation of radio refractivity structure using matched field array processing," *IEEE Trans. Antennas Propagat.* , 48, pp. 345–356, Mar. 2000.

[9] Barton, D.K., Modern radar systems analysis, Artech House, Norwood, MA, USA, 1988.
[10] Barrick, D.E., "Grazing behavior of scatter and propagation above any rough surface," IEEE Trans. Antennas and Prop., 46(1), pp. 73-83, 1998.
[11] Paulus, R.A., Practical application of an evaporation duct model, *Radio Science*, 20(4), 887-896, Jul.-Aug., 1985.
[12] Blanc, T.V., Accuracy of bulk-method-determined flux, stability, and sea surface roughness, J. of Geophysical Research, 92(C4), 3867-3876, Apr., 1987.